HHS Public Access

Author manuscript

Adv Biol Regul. Author manuscript; available in PMC 2023 January 01.

Published in final edited form as:

Adv Biol Regul. 2022 January ; 83: 100842. doi:10.1016/j.jbior.2021.100842.

Biochemical basis for an interaction between SNX27 and the flexible SNX1 N-terminus

Mintu Chandra[1,2], **Brett M. Collins**[3], **Lauren P. Jackson**[1,2,4,*]

[1]Department of Biological Sciences, Vanderbilt University, Nashville, TN, USA

[2]Center for Structural Biology, Vanderbilt University, Nashville, TN, USA

[3]Institute for Molecular Bioscience, The University of Queensland, Brisbane, QLD, 4072, Australia

[4]Department of Biochemistry, Vanderbilt University, Nashville, TN, USA

Abstract

Metazoans require the sorting nexin (SNX) protein, SNX27, to recycle hundreds of important transmembrane protein receptors from endosomes to the plasma membrane. Cargo recycling by SNX27 requires its interaction with retromer, a heterotrimer known to assemble on membranes with multiple sorting nexins, including SNX-BAR proteins and SNX3. SNX27 has also been functionally linked to SNX-BARs, but the molecular basis of this interaction has been unknown. We identify a direct biochemical interaction between the conserved and flexible SNX1/SNX2 N-terminus and full-length SNX27 using purified proteins in pulldown experiments. Sequence alignments indicate both SNX1 and SNX2 contain two short and conserved stretches of acidic residues bearing a DxF motif in their flexible N-terminal regions. Biochemical pulldown and mapping experiments reveal forty residues in the N-terminus of either SNX1 or SNX2 can mediate binding to SNX27. SNX27 truncation analysis demonstrates the SNX27 FERM domain binds the SNX1 N-terminus. Calorimetry experiments quantified binding between the SNX1 N-terminus and SNX27 in the low micromolar affinity range (K_D ~10 μM) and suggest the second DxF motif may play a more prominent role in binding. Mutation of either DxF sequence in SNX1 abrogates measurable binding to SNX27 in the calorimeter. Modelling from both predicted and experimentally determined structures suggests the SNX27 FERM domain could accommodate both DxF motifs simultaneously. Together, these data suggest SNX27 is directly linked to specific SNX-BAR proteins through binding acidic motifs in the SNX1 or SNX2 N-terminus.

*Corresponding author: lauren.p.jackson@vanderbilt.edu.

CRediT author statement

Mintu Chandra: Investigation; Methodology; Visualization Writing- Review & Editing

Brett Collins: Conceptualization; Writing- Review & Editing; Supervision; Funding acquisition

Lauren Jackson: Conceptualization; Writing- Original Draft; Writing-Review & Editing; Supervision; Funding aquisition

Conflict of interest

The authors declare no competing conflicts of interest.

Introduction

Membrane trafficking is essential for human physiology by controlling the spatiotemporal organization of transmembrane protein cargoes within cells. Endocytic events deliver transmembrane proteins and their ligands to early endosomal compartments, where cargoes can be sorted for degradation in lysosomes; retrieved via the *trans*-Golgi network (TGN); or recycled to the plasma membrane. Regulation is crucial in order to maintain the delicate balance between internalization and recycling of many different cargo proteins and is essential for controlling protein surface levels. Defects in endosomal trafficking lead to perturbed homeostasis of transmembrane proteins, which in turn are linked to a variety of patho-physiological conditions including Alzheimer's, Parkinson's disease, cancer, and diabetes[1].

The highly conserved retromer complex (VPS26/VPS35/VPS29 subunits) regulates and orchestrates multiple important cargo sorting events within the endosomal network[2–4]. In yeast, retromer is often considered a stable pentamer composed of Vps26/Vps35/Vps26 and two sorting nexin (SNX) proteins with dimeric Bin/Amphiphysin/Rvs (BAR) domains (Vps5 and Vps17)[5]. Metazoan retromer interacts with multiple sorting nexins, including SNX-BARs, SNX3, and SNX27. All SNX proteins contain PX domains, which often recognize PtdIns3-*P* headgropus enriched in endosomal membranes. In mammals, retromer associates with SNX-BAR proteins that form heterodimers (SNX1/SNX2 with SNX5/SNX6) and play critical roles in cargo retrieval and recycling from endosomes back to the TGN. The SNX1/2:SNX5/6 heterodimer is the counterpart of yeast Vps5/Vps17[5]. Reconstitution and structural studies have revealed how either yeast Vps5 homodimer[6] or yeast or mammalian SNX3[7] can assemble on membranes with retromer to generate tubules *in vitro*. In addition, mammalian SNX-BAR heterodimers have been shown to bind and sort cargo independently of retromer as the ESCPE-1 complex[8–10]. The SNX5 and SNX6 PX domains bind specific motifs found in transmembrane protein cargoes, including CI-MPR[9]. Overall, different combinations of SNX proteins with retromer promote either retrieval or recycling of specific cargoes, and mutations in multiple genes encoding these protein machineries have been shown to contribute to neurological disorders.

How SNX27 assembles with retromer remains poorly understood[4]. SNX27 is a member of the PX-FERM subfamily of sorting nexins and contains three structured domains: the N-terminal postsynaptic density 95/discs large/zonula occludens-1 (PDZ) domain; a PX domain; and the band 4.1/ezrin/radixin/moesin (FERM) domain at its C-terminus (Figure 1A). SNX27 is unique to metazoans and is required for recycling hundreds of transmembrane protein receptors[11]. Structural and biochemical data indicate the SNX27 PDZ domains binds directly to the retromer VPS26 subunit[12] and recognizes PDZ binding motifs in transmembrane protein cargoes[13]. The PX domain recognizes PI3*P*[14], while the FERM domain has been implicated in binding NPxY motifs[15] and small Ras GTPases[16]. In metazoans, SNX27/retromer is thought to function as a coat that recycles specific cargoes from endosomes to the plasma membrane. SNX27/retromer has been functionally linked to the SNX-BAR complex[11,17], but whether and how these large protein machineries bind each other directly has remained unknown.

Using biochemical and biophysical approaches, we tested whether and how two related mammalian SNX-BAR proteins (SNX1 and SNX2) recognize SNX27. We confirmed biochemically that both SNX1 and SNX2 interact directly with SNX27, and mapped binding to the SNX1 or SNX2 N-terminus and the SNX27 FERM domain. We further identified two conserved acidic binding motifs in the flexible N-terminal regions of SNX1 or SNX2; these motifs are absent in other SNX-BAR proteins. Calorimetry data revealed each acidic motif interacts independently with SNX27 FERM with low micromolar binding affinity. Both motifs are needed together for robust binding, as deletion of either motif reduces SNX1 binding affinity for SNX27 *in vitro*. This newly identified interaction of the SNX27 FERM domain with SNX1 or SNX2 directly links a metazoan-specific sorting nexin to SNX-BARs. This study raises important new questions about how SNX27 is linked to formation of SNX-BAR/retromer or to ESCPE-1 coats in cells.

Results

SNX27 directly binds the SNX1 or SNX2 flexible N-terminus

Published data using proteomic approaches[11] suggested two specific SNX-BAR family members, SNX1 and SNX2, were highly enriched in the SNX27 interactome. SNX1 and SNX2 are highly conserved (Figure S1) proteins that likely arose from a gene duplication event. We explored whether SNX27 could directly bind SNX1 (Figure 1) or SNX2 (Figure S2) using recombinant purified proteins in pulldown experiments. Both SNX1 and SNX2 contain N-terminal flexible regions (Figure S1) followed by PX and BAR domains (Figure 1; Figure S2). We first tested multiple SNX1 constructs (Figure 1) encoding full-length protein; PX-BAR (residues 143-272); or the BAR domain alone (residues 302-522). Affinity chromatography *in vitro* pulldown binding assays were used to probe the interaction between SNX27 and either full length or truncated versions of SNX1 (Figure 1B). Glutathione- S- transferase (GST)-tagged SNX27 was used as bait and His-tagged SNX1 proteins were used as prey. Either full length SNX1 or the SNX1 N-terminus alone (Figure 1B) can be pulled down by full-length SNX27. In contrast, truncated constructs containing SNX1 PX-BAR or BAR domain alone did not show detectable binding to SNX27 (Figure 1B). We further tested whether the SNX2 N-terminus (residues 1-139; Figure S2) binds full-length SNX27 and established it also associates with SNX27 *in vitro*. Together, these data suggest the flexible N-terminal regions of both SNX1 (residues 1-139) and SNX2 (residues 1-137) are capable of interacting directly with SNX27.

Two conserved acidic motifs in SNX1 are required to bind SNX27

To further define the minimal binding region, we generated seven SNX1 deletion constructs by truncating its N-terminus (Figure 2). These constructs comprised GST-tagged SNX1 residues 1–60; residues 1–70; residues 1-80; residues 1-90; residues 40-60; residues 40-70; residues 40-80; residues 40-90; and residues 40-100. Pulldown experiments were used to test whether each N-terminal construct binds SNX27. All GST-SNX1 constructs showed some binding to full-length 6xHis-SNX27 (Figure 2A), but three constructs appeared to demonstrate stronger affinity (Figure 2B) in Western blots probed with α-His: GST-SNX1 residues 1-90; residues 40-100 and residues 40-90. Comparison of two constructs (SNX1 residues 1–90 versus SNX1 residues 1–80) showed that loss of ten residues resulted in

weaker binding to SNX27. This indicates a short stretch of SNX1 amino acids (residues 80–90) make an important contribution to binding SNX27 (Figure 2). In addition, comparison between other SNX1 N-terminal deletion constructs (residues 40-60; 40-70; 40-80) further revealed a second short stretch of amino acids (residues 40–50) that also mediate SNX27 binding, albeit more weakly (Figure 2). Sequence alignments of SNX1 and SNX2 across species reveal these two N-terminal regions (residues 40–50 and 80–90) share conserved in both SNX1 and SNX2 (Figure S1). Both motifs share a similar pattern (DxF) featuring an acidic residue, any amino acid, and a hydrophobic residue; the second motif is particularly highly conserved. These data suggest the N-terminal flexible region of SNX1 binds SNX27 using two short motifs contributed by residues 40–50 and 80–90. The second motif (residues 80-90) apparently makes the greater contribution to binding.

SNX27 binds the SNX1 N-terminus using the FERM domain

SNX27 contains three folded domains (Figure 1A), so we next determined which domain mediates SNX1 binding. We generated three His6-tagged constructs comprised of individual SNX27 domains (PDZ, PX, and FERM-like domains) and assayed whether each could be bound by GST-SNX1 (residues 1-142) in pulldown assays (Figure 3). This experiment showed the SNX1 N-terminus can bind either full-length SNX27 or the SNX27 FERM domain, but neither the PDZ nor PX domains alone are sufficient to mediate the interaction *in vitro*.

SNX1 acidic motifs bind SNX27 FERM with low micromolar affinity

We next used isothermal titration calorimetry to quantify binding affinities between SNX27 and SNX1 (Figure 4). We tested each individual SNX1 motif (DIF and DLF; synthesized as peptides) and purified recombinant SNX1 protein containing both motifs. We also tested SNX1 N-terminal or motif binding to either full-length SNX27 or the FERM domain. In these experiments, recombinant purified untagged full-length SNX27 or SNX27 FERM was placed in the calorimeter cell. Either GST-SNX1 (residues 1-142) or synthesized peptides (Genscript) containing individual motifs were titrated into the cell. For experiments with GST-SNX1, a control experiment in which GST-SNX1 was titrated into buffer alone was used to subtract background heats generated by the GST dimer when titrated into the cell. Overall, data indicate the SNX1 N-terminus binds either full-length SNX27 or FERM domain with a low micromolar K_D (10-12 μM) typical of interactions between trafficking proteins. Either peptide on its own exhibits weaker binding. The first motif (SNX1 residues 40-50) appears two-fold weaker, while the second motif (SNX1 residues 80-90) is only slightly weaker than binding to the full SNX1 N-terminus. These data agree with pulldown experiments (Figure 2) and suggest the second motif may play a role in ensuring robust binding to SNX27 FERM.

Discussion

In this work, we use biochemical and biophysical approaches to identify the SNX1 or SNX2 N-terminus as new binding partners for the SNX27 FERM domain. While our work was in progress, two other groups independently identified this interaction[18,19] using orthogonal approaches. Yong and colleagues[18] very recently determined an X-ray crystal structure

of the SNX27 FERM linked covalently to a DxF motif (PDB: 7CT1). This structure identified a hydrophobic cavity surrounded by basic residues on the SNX27 FERM domain that accommodates one DxF motif, and this binding pocket was further validated using calorimetry.

The calorimetry data presented here (Figure 4) suggest the presence of both DxF motifs provides the highest affinity binding between SNX1 and the SNX27 FERM domain. One interpretation of these data is that SNX27 FERM may contain a second binding site for the second motif. We note there is a second hydrophobic pocket flanked by basic residues located on the opposite side of the FERM domain (Figure 5C, 5D). Modeling of full-length SNX1 using AlphaFold2 (Figure 5B) suggests the two motifs are separated by approximately 50 Å, which represents sufficient distance to span the FERM domain and allow both SNX1 DxF motifs to bind simultaneously. AlphaFold2 predicts the binding site on the SNX27 F3 sub-domain[19], which has been observed in the co-crystal structure[18]. In contrast, AlphaFold2 did not identify the putative binding site on the F1 sub-domain (not shown), so it will be important to test this prediction experimentally. Another interpretation of the ITC data is that the presence of two motifs will increase the avidity of the interaction to ensure SNX27 can engage SNX1 at the right time and place.

Overall, multiple recent studies identify a new interaction between SNX1 and SNX27, and we further confirm an interaction between SNX27 and SNX2. These discoveries give rise to multiple fascinating and unresolved questions. For example, can SNX27 engage both retromer and SNX1 (or SNX2) simultaneously on membranes? Multiple studies have firmly linked SNX27 with endosomal recycling[20,21] and with retromer[11–13,22]. SNX27/retromer has thus been proposed to form a membrane-associated coat[2,23] to recycle specific endosomal cargoes. SNX27 is now biochemically linked to the SNX-BAR proteins (SNX1 and SNX2), which are also linked directly to retromer coat formation on membranes[6]. It is possible that SNX27 forms a “super-complex” with both SNX-BARs and retromer[18]. However, it remains unclear how membrane-associated SNX-BAR/retromer coats accommodate SNX27 in current structural models[6,7]. The SNX27 PDZ domain binds VPS26, which forms dimers on top of BAR (Vps5) dimers in reconstituted SNX-BAR/retromer coats[6]. How then does SNX27 recognize or access PDZ cargoes in the membrane? Furthermore, cargoes recognized by SNX27/retromer and SNX-BAR/retromer coats have been proposed to follow different trafficking itineraries[3,22,24], with SNX27 cargoes being recycled to the plasma membrane while SNX-BAR/retromer cargoes returning to the TGN. However, more recent data[18] suggest SNX27 works together with SNX-BARs to recycle cargoes like GLUT1. This and other work may implicate the N-termini of SNX-BARs in regulating cargo itineraries depending on wither SNX27 is present or absent.

Alternatively, it is possible that SNX27 may engage SNX-BARs and retromer in independent or sequential events. Mammalian SNX1/SNX5 has been proposed to function as a distinct coat called ESCPE-1, which mediates cargo sorting to the TGN independently of retromer[9]. The specific role of the SNX2/SNX6 heterodimer in endosomal trafficking remains unclear; SNX6 can recognize CI-MPR but appears to bind other cargoes less efficiently[9]. Biochemical presented here suggest SNX27 can bind either SNX1 or SNX2. Could SNX27 engage SNX-BAR heterodimers to promote tubulation of cargoes bearing

PDZ motifs? Perhaps both SNX27 and SNX-BARs require retromer to function as a scaffold to link together or further concentrate these assemblies. Ongoing structural and biochemical studies are required to uncover how sorting nexins and retromer assemble to orchestrate the complex trafficking itineraries on endosomal membranes.

Materials and Methods

Chemicals and reagents.

All chemicals were purchased from ThermoFisher unless otherwise noted. SNX1 peptides containing DxF motifs (residues 40-50, DTEGE**DIF**TGA, and residues 80-90, EQDQEPQ**DLF**A) used for calorimetry experiments were synthesized by Genscript.

Molecular biology and cloning.

DNA encoding full-length human SNX27, SNX1, and SNX2 proteins optimized for *Eschericia coli* expression were synthesized by Genscript Corporation (USA), and subsequently cloned into either pET28A or pGEX-4T-2 vectors for expression as N-terminal 6xHis or GST fusion proteins. SNX27_PDZ, SNX27_PX, SNX27_FERM domains, SNX1_PX-BAR and SNX1_BAR domains were sub-cloned into the pET28A vector for expression as N-terminal His fusion proteins. SNX1_N-terminal (1-142 aa), SNX1_N-terminal (1-60 aa), SNX1_N-terminal (1-70 aa), SNX1_N-terminal (1-80 aa), SNX1_N-terminal (1-90 aa), SNX1_N-terminal (1-100 aa), SNX1_N-terminal (40-60 aa), SNX1_N-terminal (40-70 aa), SNX1_N-terminal (40-80 aa), SNX1_N-terminal (40-90 aa), SNX1_N-terminal (40-100 aa) and SNX2_N-terminal (1-139 aa) domains were sub-cloned into the pGEX4T2 vector for expression as N-terminal GST fusion proteins. The DxF motifs were mutated to alanine residues using the QuikChange II site-directed mutagenesis protocol (Stratagene).

Recombinant protein expression and purification.

The plasmid encoding 6xHis-tagged SNX27_FL (1-541 aa), SNX27_PDZ (43-136 aa), SNX27_PX (161-269 aa), SNX27_FERM (273-525 aa), SNX1_FL (1-522 aa), SNX1_PX-BAR (143-522 aa), SNX1_BAR (302-522 aa) and GST-fusion SNX27_FL (1-541 aa), SNX1_N-terminal (1-142 aa), SNX1_N-terminal (1-60 aa), SNX1_N-terminal (1-70 aa), SNX1_N-terminal (1-80 aa), SNX1_N-terminal (1-90 aa), SNX1_N-terminal (1-100 aa), SNX1_N-terminal (40-60 aa), SNX1_N-terminal (40-70 aa), SNX1_N-terminal (40-80 aa), SNX1_N-terminal (40-90 aa), SNX1_N-terminal (40-100 aa) and SNX2_N-terminal (1-139 aa) were transformed into BL21(DE3)/pLysS *E. coli* cells (Promega), and expressed in LB broth at 37 °C until A_{600} reached 0.8. Cultures were induced with 0.5 mM isopropyl 1-thio-β-D-galactopyranoside (IPTG, Research Products International) and allowed to grow at 20 °C overnight, and cells were harvested by centrifugation (6000 × *g*, 10 min, 4 °C). The cell pellet was resuspended in lysis buffer (50 mM Tris (pH 8.0), 300 mM NaCl, 50 μg/ml of benzamidine, 100 units DNaseI, and 2 mM β-mercaptoethanol). The cells were lysed by mechanical disruption at 30 kpsi using a cell disrupter (Constant Systems). The lysate was clarified by centrifugation at 50,000 × *g* for 30 min at 4 °C. Proteins were purified using affinity chromatography from the clarified lysate. For His-tagged constructs, the purification was performed on a NI-NTA (GE Healthcare) gravity column and for

GST-tagged constructs, the purification was performed on a glutathione–Sepharose (GE Healthcare) gravity column. The His-tagged proteins were eluted in 50 mM Tris (pH 8.0), 300 mM NaCl, and 250 mM imidazole. The GST-tagged proteins were eluted in 50 mM Tris (pH 8.0), 300 mM NaCl, and 20 mM reduced glutathione. The eluted affinity purified proteins were finally subjected to size exclusion chromatography using a superdex-200 16/600 Hiload column, pre-equilibrated with 50 mM Tris (pH 8.0), 100 mM NaCl and 2 mM DTT, attached to an AKTA pure (GE Healthcare). The purified proteins were concentrated to 8-10 mg/ml using a Centricon Ultra-10 kDa centrifugal filter (Millipore, USA) for pull down and ITC experiments. The concentration of proteins were determined by the Bio-Rad Protein Assay (Bio-Rad, USA) after each purification step.

GST pull down experiments.

1 nmol GST-tagged proteins (either GST-SNX27_FL or GST-SNX1_N-terminal (1-142) or SNX1_N-terminal (1-60 aa) or SNX1_N-terminal (1-70 aa) or SNX1_N-terminal (1-80 aa) or SNX1_N-terminal (1-90 aa) or SNX1_N-terminal (1-100 aa) or SNX1_N-terminal (40-60 aa) or SNX1_N-terminal (40-70 aa) or SNX1_N-terminal (40-80 aa) or SNX1_N-terminal (40-90 aa) or SNX1_N-terminal (40-100 aa) or GST-SNX2_N-terminal (1-139) were mixed with 1 nmol of His-tagged proteins (either SNX1_FL or SNX1_PX-BAR or SNX1_BAR or SNX27_FL or SNX27_PDZ or SNX27_PX or SNX27_FERM), for 1 hr at 4°C. Protein mixture was then centrifuged at high speed to remove any precipitated proteins. The supernatant was then added to glutathione Sepharose pre-equilibrated in 20 mM Tris (pH 8.0), 300 mM NaCl, 1 mM DTT (Research Products International) and allowed to mix for 30 minutes at 4°C. Beads were washed five times in the above buffer supplemented with 0.5% Triton-X100 (Sigma Aldrich). Bound proteins were analyzed by SDS-PAGE and Western blots using HRP conjugated mouse anti-His antibody (Abcam) with 1:8000 dilution.

Isothermal titration calorimetry (ITC).

ITC measurements were conducted on a Nano-ITC instrument (TA Instruments) in buffer consisting of 20 mM Tris (pH 8.0), 100 mM NaCl and 2 mM DTT. SNX1 peptides were dissolved in 20 mM Tris, pH 8, 100 mM NaCl and 2 mM DTT for use in ITC binding experiments with either full length SNX27 or SNX27_FERM domain proteins. In a typical experimental setup, the sample cell was filled with 300 μL of SNX27_FL or SNX27_FERM domain protein. The syringe contained a 50 μL analyte solution of wild-type of AAA mutant SNX1 synthetic peptides (residues 40-50, DTEGE**DIF**TGA; or residues 80-90, EQDQEPQ**DLF**A) or the SNX1 N-terminus. All solutions were degassed prior to being loaded into the cell. Aliquots (2 μL) of 1 mM analyte solutions from the syringe were injected into a 50 μM SNX27_FL or SNX27_FERM domain protein solution at 25°C within an interval gap of 3 minutes with the syringe rotating at 150 rpm to ensure proper mixing. Heats of dilution were measured by injecting analytes into buffer and subtracted from the heat of interaction. Data were analyzed using Nanoanalyser software (TA Instruments) to extract the thermodynamic parameters, $\Delta H°$, K_d ($1/K_a$), and stoichiometry (n). The dissociation constant (K_d), enthalpy of binding ($\Delta H°$), and stoichiometry (n) were obtained after fitting the integrated and normalized data to a single-site binding model. The apparent binding free energy ($\Delta G°$) and entropy ($\Delta S°$) were calculated from the relationships $\Delta G° =$

$RTln(K_d)$ and $\Delta G° = \Delta H° - T\Delta S°$. All experiments were performed in triplicate to ensure reproducibility; standard deviations are reported from three runs.

Sequence alignments.

Representative metazoan SNX1 and SNX2 sequences were aligned using MultiAlign[25]. The following species were used in alignments: *C. elegans, A. thaliana, D. melanogaster, D. rerio, X. laevis, M. musculus*, and *H. sapiens*.

Supplementary Material

Refer to Web version on PubMed Central for supplementary material.

Acknowledgements

MC generated all biochemical and calorimetry data. MC generated figures, and LPJ wrote the paper with input from all authors. This project was conceived by MC and BMC: initial biochemical experiments were conducted in the lab of BMC, and mapping and calorimetry experiments were completed in the lab of LPJ. MC and LPJ are supported by NIH R35GM119525. BMC is supported by the Australian National Health and Medical Research Council (NHMRC) (APP1156493, APP1136021). The authors declare no competing conflicts of interest.

References

1. McMillan KJ, Korswagen HC & Cullen PJ The emerging role of retromer in neuroprotection. Curr. Opin. Cell Biol 47, 72–82 (2017). [PubMed: 28399507]
2. Burd CG & Cullen PJ Retromer: a master conductor of endosome sorting. Cold Spring Harb Perspect Biol 6, (2014).
3. Gallon M & Cullen PJ Retromer and sorting nexins in endosomal sorting. Biochem. Soc. Trans 43, 33–47 (2015). [PubMed: 25619244]
4. Chandra M, Kendall AK & Jackson LP Toward Understanding the Molecular Role of SNX27/Retromer in Human Health and Disease. Front. Cell Devel Biol 9, 642378 (2021). [PubMed: 33937239]
5. Horazdovsky BF et al. A sorting nexin-1 homologue, Vps5p, forms a complex with Vps17p and is required for recycling the vacuolar protein-sorting receptor. Mol Biol Cell 8, 1529–41 (1997). [PubMed: 9285823]
6. Kovtun O et al. Structure of the membrane-assembled retromer coat determined by cryoelectron tomography. Nature 561, 561–564 (2018). [PubMed: 30224749]
7. Leneva N, Kovtun O, Morado DR, Briggs JAG & Owen DJ Architecture and mechanism of metazoan retromer:SNX3 tubular coat assembly. Sci. Adv 7, (2021).
8. Simonetti B, Danson CM, Heesom KJ & Cullen PJ Sequence-dependent cargo recognition by SNX-BARs mediates retromer-independent transport of CI-MPR. J Cell Biol 216, 3695–3712 (2017). [PubMed: 28935633]
9. Simonetti B et al. Molecular identification of a BAR domain-containing coat complex for endosomal recycling of transmembrane proteins. Nat Cell Biol 21, 1219–1233 (2019). [PubMed: 31576058]
10. Evans AJ, Daly JL, Anuar ANK, Simonetti B & Cullen PJ Acute inactivation of retromer and ESCPE-1 leads to time-resolved defects in endosomal cargo sorting. J Cell Sci 133, (2020).
11. Steinberg F et al. A global analysis of SNX27-retromer assembly and cargo specificity reveals a function in glucose and metal ion transport. Nat Cell Biol 15, 461–71 (2013). [PubMed: 23563491]
12. Gallon M et al. A unique PDZ domain and arrestin-like fold interaction reveals mechanistic details of endocytic recycling by SNX27-retromer. Proc. Natl. Acad. Sci. U. S. A 111, E3604–13 (2014). [PubMed: 25136126]

13. Clairfeuille T et al. A molecular code for endosomal recycling of phosphorylated cargos by the SNX27-retromer complex. Nat. Struct. Mol. Biol 23, 921–932 (2016). [PubMed: 27595347]
14. Chandra M et al. Classification of the human phox homology (PX) domains based on their phosphoinositide binding specificities. Nat Commun 10, 1528 (2019). [PubMed: 30948714]
15. Ghai R et al. Phox homology band 4.1/ezrin/radixin/moesin-like proteins function as molecular scaffolds that interact with cargo receptors and Ras GTPases. Proc Natl Acad Sci U S A 108, 7763–8 (2011). [PubMed: 21512128]
16. Ghai R & Collins BM PX-FERM proteins: A link between endosomal trafficking and signaling? Small GTPases 2, 259–263 (2011). [PubMed: 22292128]
17. Yong X et al. Mechanism of cargo recognition by retromer-linked SNX-BAR proteins. PLoS Biol 18, e3000631 (2020). [PubMed: 32150533]
18. Yong X et al. SNX27-FERM-SNX1 complex structure rationalizes divergent trafficking pathways by SNX17 and SNX27. Proc Natl Acad Sci U S A 118, (2021).
19. Simonetti B, Guo Q, Gimenez-andres M & Chen K Mechanistic basis for SNX27-Retromer coupling to ESCPE-1 in promoting endosomal cargo recycling . bioRxiv 2021.08.28, (2021).
20. Lunn M-L et al. A unique sorting nexin regulates trafficking of potassium channels via a PDZ domain interaction. Nat. Neurosci 10, 1249–59 (2007). [PubMed: 17828261]
21. Lauffer BEL et al. SNX27 mediates PDZ-directed sorting from endosomes to the plasma membrane. J Cell Biol 190, 565–74 (2010). [PubMed: 20733053]
22. Temkin P et al. SNX27 mediates retromer tubule entry and endosome-to-plasma membrane trafficking of signalling receptors. Nat. Cell Biol 13, 715–21 (2011). [PubMed: 21602791]
23. Simonetti B & Cullen PJ Endosomal Sorting: Architecture of the Retromer Coat. Curr. Biol 28, R1350–R1352 (2018). [PubMed: 30513333]
24. Choy RW-Y et al. Retromer mediates a discrete route of local membrane delivery to dendrites. Neuron 82, 55–62 (2014). [PubMed: 24698268]
25. Corpet F Multiple sequence alignment with hierarchical clustering. Nucleic Acids Res 16, 10881–90 (1988). [PubMed: 2849754]

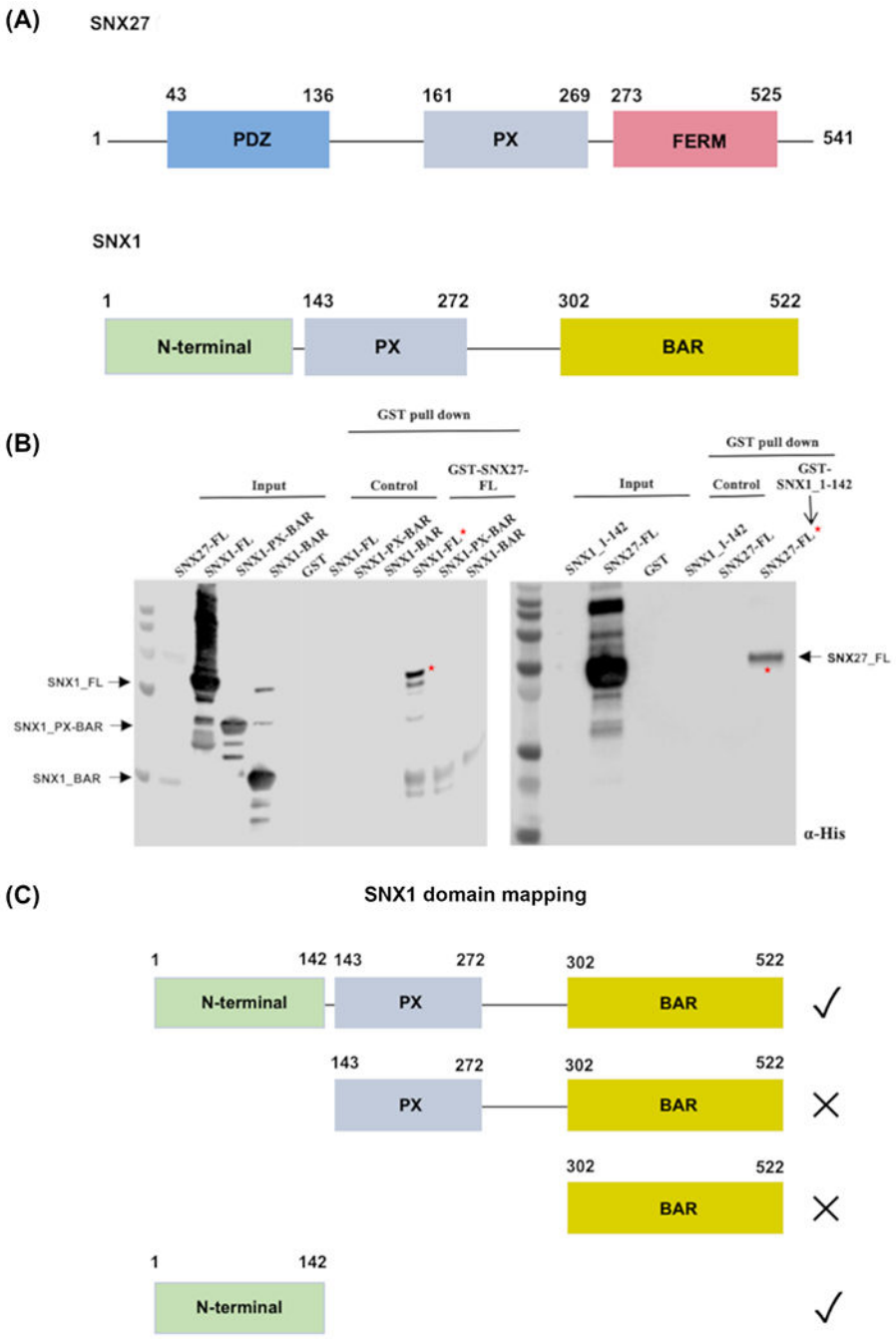

Figure 1. The flexible SNX1 N-terminus binds full-length SNX27 *in vitro*.

(A) Domain schematics of SNX27 and SNX1. SNX27 contains an N-terminal PDZ domain (light blue), middle PX domain (grey), and C-terminal FERM-like domain (purple). The FERM domain is further divided into F1, F2, and F3 sub-domains (not shown). SNX1/SNX2 contains a flexible N-terminal region followed by PX and BAR domains. (B) Pulldown assays were conducted using purified SNX27 and SNX1 proteins; Western blots were probed with anti-His (Abcam). The left-hand blot shows GST-tagged full-length SNX27 as bait and His-tagged SNX1 constructs (see text) as prey. GST-SNX27 pulls down full-length

SNX1, but not constructs containing either SNX1 PX-BAR or SNX1 BAR domain alone. The right-hand blot demonstrates that GST-SNX1 (residues 1-142) pulls down full-length SNX27. (C) Summary of pulldown binding data.

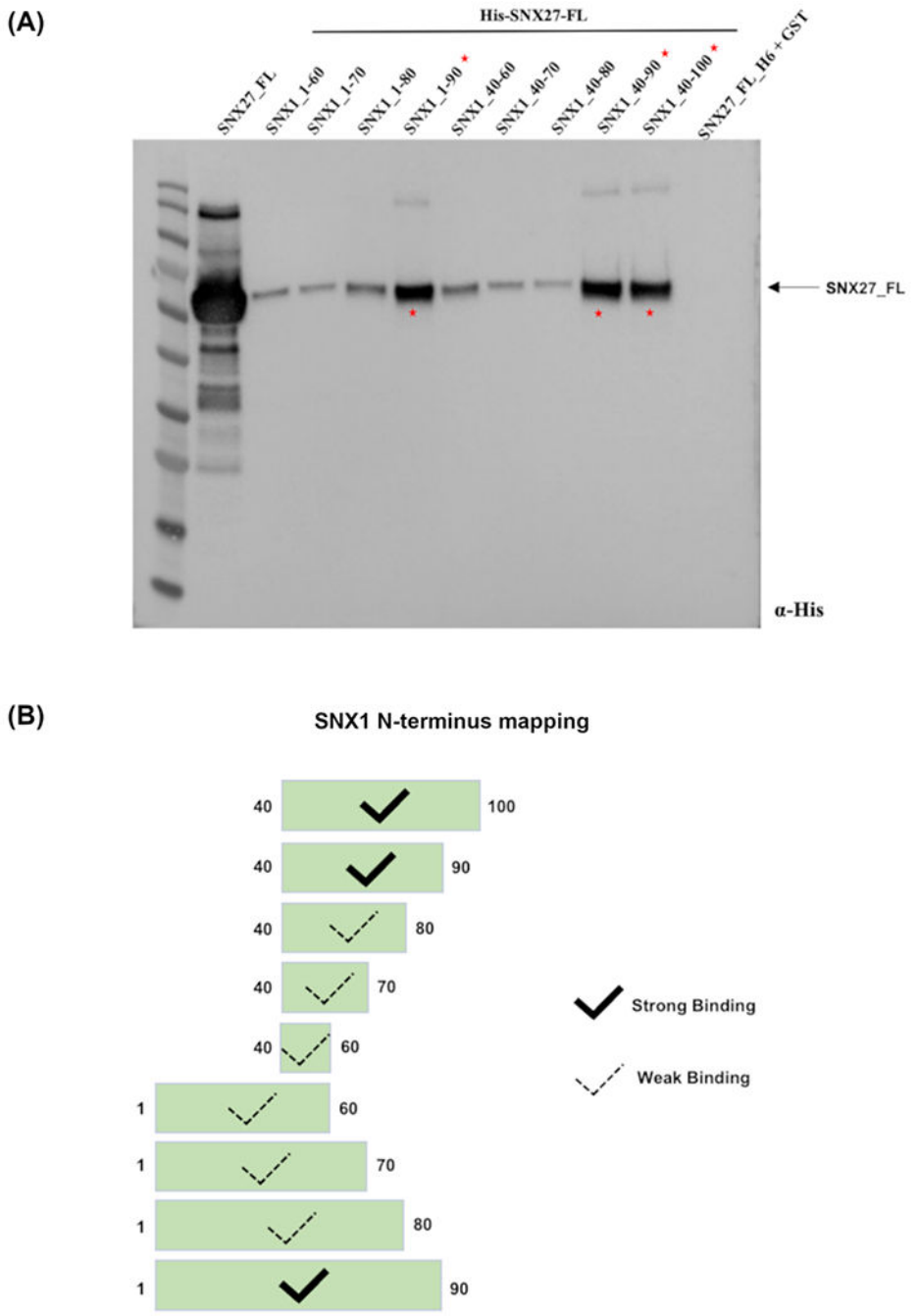

Figure 2. Two short regions in SNX1 mediate binding to SNX27.

(A) Biochemical mapping experiments define two regions in the SNX1 N-terminus that bind full-length SNX27. Purified GST-SNX1 and H6-SNX27 proteins were used in pulldown experiments; a Western blot probed with anti-His is shown. Three GST-tagged SNX1 constructs exhibit robust binding to full-length H6-SNX27: GST-SNX1 (residues 1-90); GST-SNX1 (residues 40-90); and GST-SNX1 (residues 40-100). (B) Schematic summary of SNX1/SNX27 pulldown binding data.

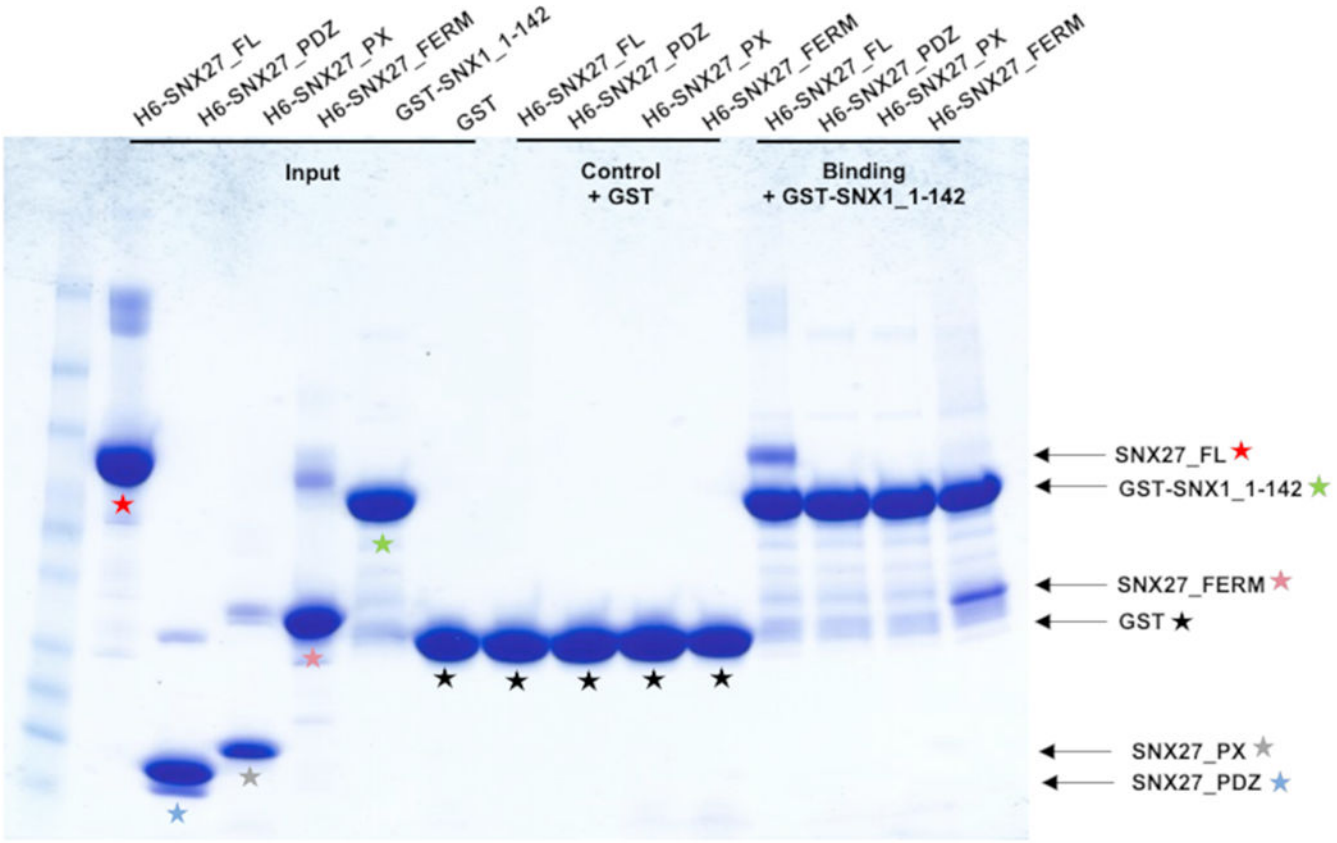

Figure 3. The SNX27 FERM domain mediates binding to SNX1.

Pulldown mapping experiments using purified GST-SNX1 N-terminus (residues 1-142) and H6-SNX27 proteins (PDZ, PX, or FERM) domains; SDS-PAGE gel stained with Coomassie blue. GST-SNX1 shows binding to either full-length SNX27 or to the SNX27 FERM domain. Colored stars denote different SNX27 and SNX1 constructs and match corresponding domains shown in Figure 1A.

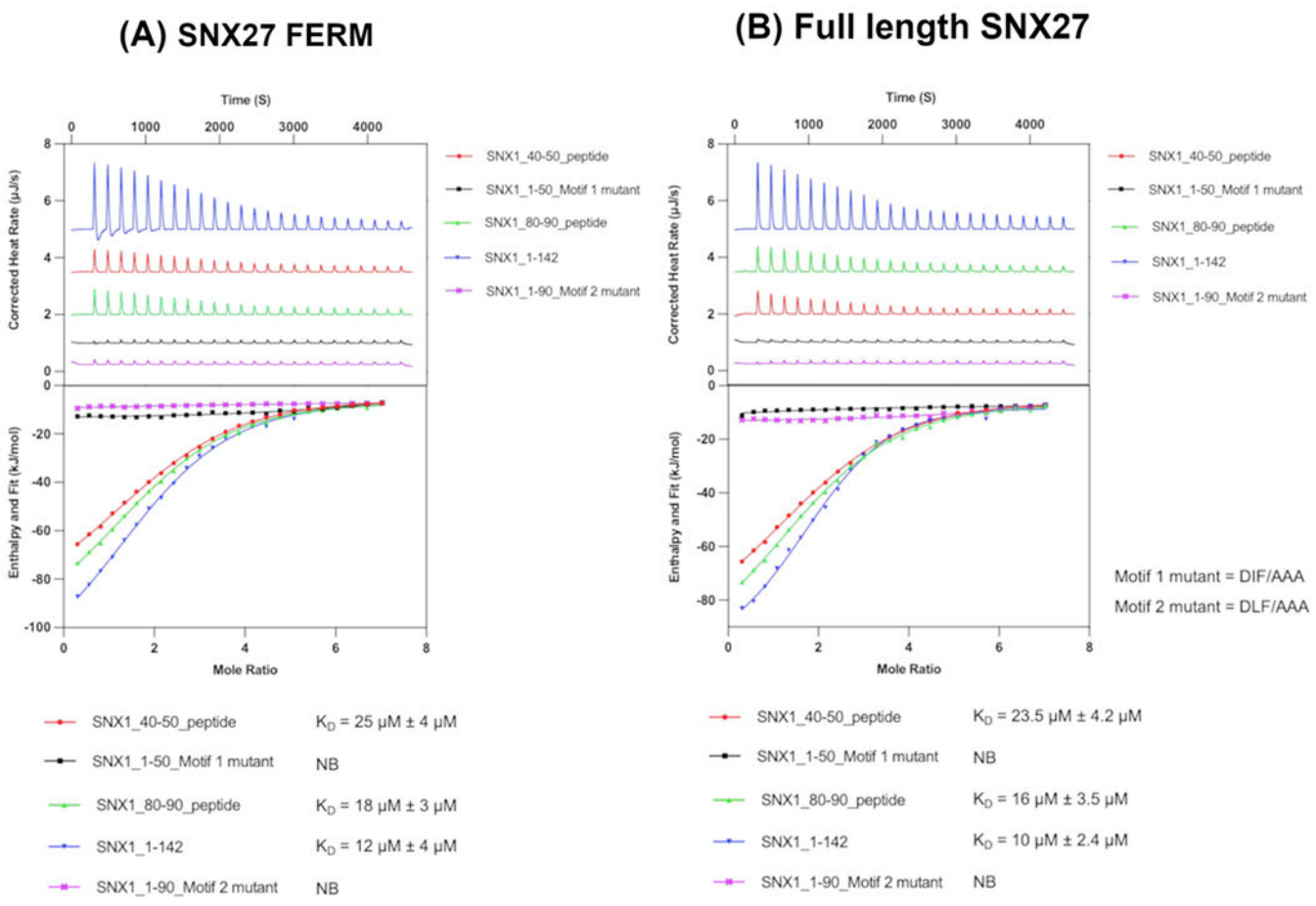

Figure 4. Two acidic motifs in SNX1 mediate binding to SNX27.

(A) Representative isotherms of SNX27 FERM domain with the SNX1 N-terminus (residues 1-142) and SNX1 peptides representing the first (SNX1 residues 40-50) or second (SNX1 residues 80-90) acidic DxF motifs. SNX1 N-terminus binds SNX27 FERM domain with a low micromolar K_D (12 µM). Mutation of either DxF sequence to AAA abrogates measurable binding (denoted "NB") to SNX27 FERM in the calorimeter. ITC experiments were conducted three times to generate reported standard deviation values. (B) Representative isotherms of full-length SNX27 with the SNX1 N-terminus (residues 1-142) and SNX1 peptides representing the first (SNX1 residues 40-50) or second (SNX1 residues 80-90) acidic DxF motifs. As with the FERM domain, mutation of the DxF sequence to AAA abrogates measurable binding. Together, these data further suggest the FERM domain mediates binding to SNX1. Both motifs bind SNX27, and the second DLF motif appears to play the predominant role.

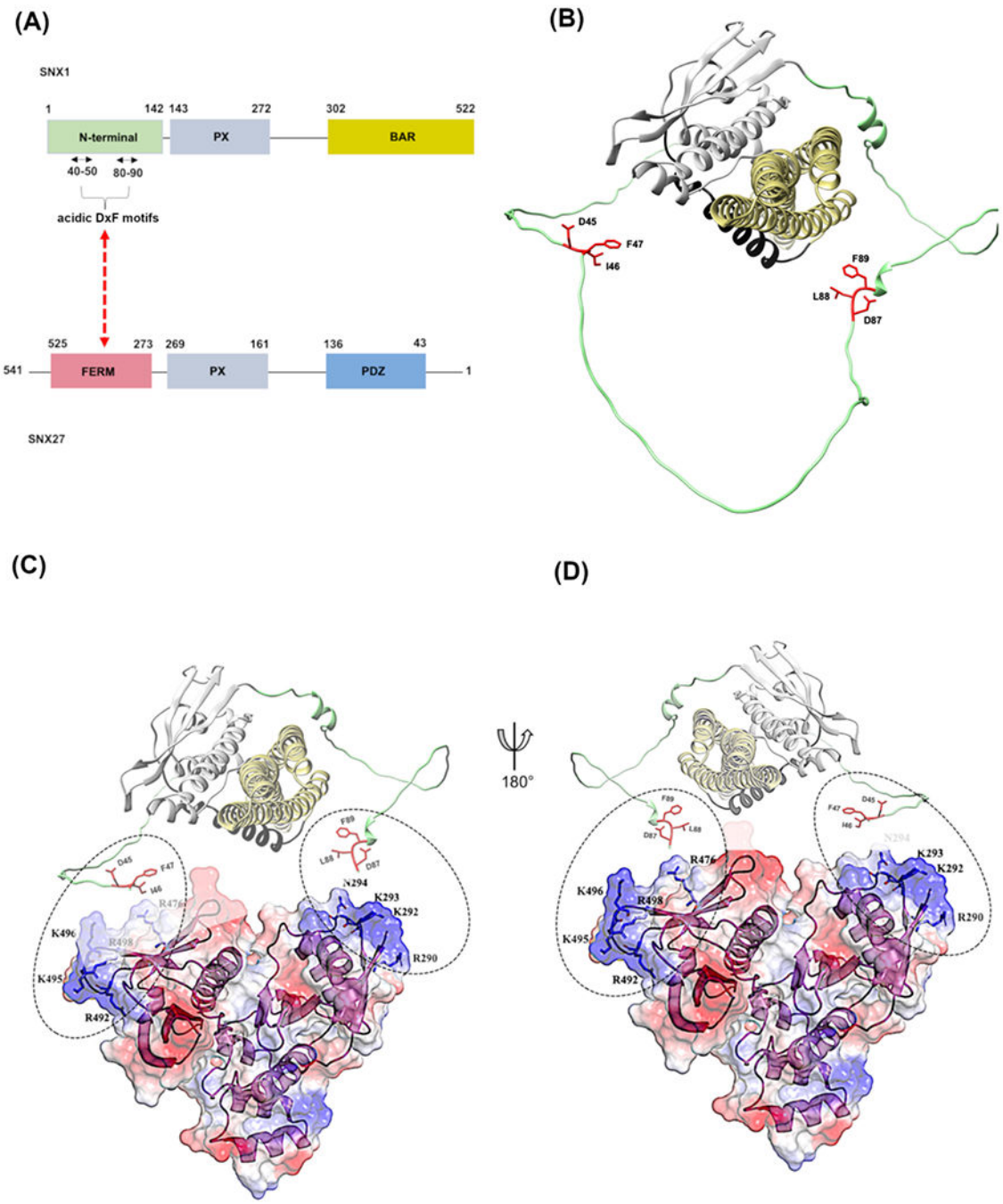

Figure 5. Modelling the SNX1/SNX27 interaction.

(A) Domain schematics of SNX1 and SNX27 showing the newly identified interaction. (B) Model of full-length SNX1 generated using AlphaFold2; the two acidic motifs (DIF and DLF) found in the flexible N-terminus are highlighted as sticks. (C, D) Two different views of the SNX27 FERM domain (PDB: 7CT1) modeled with SNX1 acidic motifs. The left-land view (C) shows SNX1 in the same orientation as panel (B). The right-hand (D) view shows SNX1 rotated by 180 degrees. An X-ray crystal structure using a fusion construct revealed a DLF motif binds the SNX27 FERM pocket composed of a hydrophobic groove with

surrounding basic (R492, K496, R498) residues; this is similar to the view shown in (D). There is a second location on SNX27 FERM that contains a hydrophobic groove with flanking basic residues (R290, K292, K293). Both pockets are shown in dashed circles. The second proposed pocket should be tested to determine whether it could allow both motifs to bind simultaneously (discussed further in text).